that membrane-bound HLA-G molecules are able to inhibit alloreactive NK cells with both NK1 and NK2 specificity. The basis for the discrimination between HLA-C locus alleles is a dimorphism involving residues 77 and 80 in the α1 domain of the molecule (*16*), and recent work has pinpointed the importance of amino acid residue 80 for the specificity of this recognition (*27*). The combination of Asn^{77}-Thr^{80} that is present in HLA-G can be found in some HLA-Bw4 but not HLA-C locus alleles. The fact that HLA-G binds to HLA-C–specific inhibitory receptors whereas HLA-B locus alleles do not indicates that other polymorphisms must influence HLA class I–NKIR interactions. Within this region, Met^{76} (Val^{76} in C locus and Glu^{76} in B locus alleles) and Gln^{79} (Arg^{79} in B and C locus alleles) are unique to HLA-G (Fig. 1D). It is possible that this unusual combination of amino acids enables the molecule to interact with both NK1- and NK2-specific receptors. HLA-G is more polymorphic than originally thought (*28*, *29*), but none of the reported amino acid changes involve the above-described segment of the α1 domain, which perhaps indicates the importance of this region.

The data presented here prove that at a functional level HLA-G is able to protect target cells from destruction by NK1- and NK2-specific effector cells. Whether HLA-G can also react with the p70-NKB1 family of NK cell receptors is unclear. Given that on average 14% of the $CD56^+$ cells are $NKB1^+$ (*21*) and that the overwhelming majority of these cells will also express at least one HLA-C–specific inhibitory receptor (*23*, *30*), this interaction may not be necessary to protect trophoblast cells from NK cell–mediated lysis. If a surrogate molecule replacing classical class I MHC molecules can interact with one major subclass of NK receptors, it will inactivate the majority of NK cells with which it comes into contact. Undoubtedly, the expression of HLA-G alone can fulfill these requirements, and thus molecule can function to protect cytotrophoblast cells from destruction by maternal NK cells.

REFERENCES AND NOTES

1. W. P. Faulk and A. Temple, *Nature* **262**, 799 (1976).
2. C. W. G. Redman, A. J. McMichael, G. M. Stirrat, C. A. Sunderland, A. Ting, *Immunology* **52**, 457 (1984).
3. S. A. Ellis, I. L. Sargent, C. W. G. Redman, A. J. McMichael, *ibid.* **59**, 595 (1986).
4. S. A. Ellis, M. S. Palmer, A. J. McMichael, *J. Immunol.* **144**, 731 (1990); S. Kovats *et al.*, *Science* **248**, 220 (1990).
5. D. E. Geraghty, B. H. Koller, H. T. Orr, *Proc. Natl. Acad. Sci. U.S.A.* **84**, 9145 (1987).
6. G. T. Colbern, M. H. Chiang, E. K. Main, *Am. J. Obstet. Gynecol.* **170**, 1244 (1994).
7. H. G. Ljunggren and K. Karre, *Immunol. Today* **11**, 237 (1990).
8. R. J. Natuk and R. M. Welsh, *J. Immunol.* **138**, 877 (1988).
9. A. King *et al.*, *ibid.* **156**, 2068 (1996).
10. A. King and Y. W. Loke, *Immunol. Today* **12**, 432 (1991).
11. C. M. Schmidt and H. T. Orr, *Crit. Rev. Immunol.* **13**, 207 (1993).
12. I. J. Stewart, *J. Anat.* **139**, 627 (1984); P. M. Starkey, I. L. Sargent, C. W. G. Redman, *Immunology* **65**, 129 (1988).
13. A. King, V. Wellings, L. Gardner, Y. W. Loke, *Hum. Immunol.* **24**, 195 (1989).
14. G. Chumbley, A. King, K. Robertson, N. Holmes, Y. W. Loke, *Cell. Immunol.* **155**, 312 (1994).
15. G. Deniz, S. E. Christmas, R. Brew, P. M. Johnson, *J. Immunol.* **152**, 4255 (1994).
16. M. Colonna *et al.*, *Proc. Natl. Acad. Sci. U.S.A.* **89**, 7983 (1992).
17. M. Colonna, G. Borsellino, M. Falco, G. B. Ferrara, J. L. Strominger, *ibid.* **90**, 12000 (1993).
18. M. Colonna and J. Samaridis, *Science* **268**, 405 (1995).
19. N. Wagtmann *et al.*, *Immunity* **2**, 439 (1995).
20. M. Cella, A. Longo, G. B. Ferrara, J. L. Strominger, M. Colonna, *J. Exp. Med.* **180**, 1235 (1994).
21. A. D'Andrea *et al.*, *J. Immunol.* **155**, 2306 (1995).
22. M. Vitale, S. Sivori, D. Pende, L. Moretta, A. Moretta, *Proc. Natl. Acad. Sci. U.S.A.* **92**, 3536 (1995).
23. L. L. Lanier *et al.*, *J. Immunol.* **154**, 3320 (1995).
24. J. H. Gong, G. Maki, H. G. Klingerman, *Leukemia* **8**, 652 (1994).
25. H. T. Reyburn, unpublished observations.
26. L. Pazmany *et al.*, data not shown.
27. O. Mandelboim *et al.*, *J. Exp. Med.* **184**, 913 (1996).
28. P. S. J. Morales *et al.*, *Immunogenetics* **38**, 323 (1993).
29. K. van der Ven and C. Ober, *J. Immunol.* **153**, 5628 (1994).
30. N. Wagtmann, S. Rajagopalan, C. C. Winter, M. Peruzzi, E. O. Long, *Immunity* **3**, 801 (1995).
31. Y. Takebe *et al.*, *Mol. Cell. Biol.* **8**, 466 (1988).
32. The original publication of the HLA-G cDNA derived from the BeWo choriocarcinoma cell line (*4*) contains an editing error. Repeated sequencing of the modified expression vector showed that the gac codons at amino acid positions 247 and 248 were duplicated. There is only one gac codon here, translating to one D instead of two in the original publication. Consequently, the numbering of the rest of the amino acids changes by one.
33. I. Melero, A. Salmeron, M. A. Balboa, J. Aramburu, M. Lopez-Botet, *J. Immunol.* **152**, 1662 (1994).
34. A. Moretta *et al.*, *J. Exp. Med.* **178**, 597 (1993).

35. Supported by NHI research grant CA-47554. L.P. is the recipient of a postdoctoral fellowship from the Arthritis Foundation, O.M. is a European Molecular Biology Organization fellowship scholar. H.T.R. is supported by a Wellcome Trust International Prize Travelling Research Fellowship. We thank S. A. Ellis for the HLA-G cDNA clone and B. Rybalov for technical assistance.

15 May 1996; accepted 23 August 1996

Decreased Resistance to Bacterial Infection and Granulocyte Defects in IAP-Deficient Mice

Frederik P. Lindberg,* Daniel C. Bullard, Tony E. Caver, Hattie D. Gresham, Arthur L. Beaudet, Eric J. Brown

Granulocyte [polymorphonuclear leucocyte (PMN)] migration to sites of infection and subsequent activation is essential for host defense. Gene-targeted mice deficient for integrin-associated protein (IAP, also termed CD47) succumbed to *Escherichia coli* peritonitis at inoccula survived by heterozygous littermates. In vivo, they had an early defect in PMN accumulation at the site of infection. In vitro, $IAP^{-/-}$ PMNs were deficient in β_3 integrin–dependent ligand binding, activation of an oxidative burst, and Fc receptor–mediated phagocytosis. Thus, IAP plays a key role in host defense by participating both in PMN migration in response to bacterial infection and in PMN activation at extravascular sites.

PMNs are terminally differentiated cells essential for host defense against infectious diseases. Genetic abnormalities in PMN effector functions prove that they are essential for normal host defense (*1*, *2*). At the same time, the highly destructive potential of PMNs must be strictly controlled to avoid nonspecific tissue damage. Not surprisingly, a large array of regulatory steps governs the emigration and activation of these cells, ensuring full activation of antibacterial effector functions at a site of infection, while maintaining a quiescent, inactive state in the blood stream. PMNs come into contact with extracellular matrix (ECM) when they have extravasated but not while they are in the circulation. Thus, ECM-binding integrins are ideally suited to mediate PMN activation signals specific to extravascular sites.

IAP (CD47) is an immunoglobulin (Ig) family member with a multiply membrane-spanning domain and a short cytoplasmic tail (*3*, *4*). It is physically and functionally

F. P. Lindberg and E. J. Brown, Departments of Infectious Diseases and Molecular Microbiology, Washington University School of Medicine, St. Louis, MO 63110, USA.
D. C. Bullard, Department of Molecular and Human Genetics, Baylor College of Medicine, Houston, TX 77030, USA.
T. E. Caver, Department of Molecular Microbiology and Immunology, University of Missouri School of Medicine, Columbia, MO 65212, USA.
H. D. Gresham, Research Service, Harry S. Truman Veterans Affairs Medical Center, Columbia, MO 65201, USA.
A. L. Beaudet, Department of Molecular and Human Genetics and Howard Hughes Medical Institute, Baylor College of Medicine, Houston, TX 77030, USA.

*To whom correspondence should be addressed.

associated with β_3 integrins and is expressed on virtually all cells, including erythrocytes, which lack integrins (*5*, *6*). Studies with human cells using antibodies to IAP (anti-IAP) suggest that a signaling complex between IAP and PMN β_3 integrins is required for activation of the oxidative burst and IgG Fc receptor–mediated phagocytosis by ECM proteins [such as vitronectin (*5*, *7*, *8*)], as well as by the model peptide ligand KGAGDVA (K, Lys; G, Gly; A, Ala; D, Asp; V, Val) (*9*). In addition, anti-IAP inhibits PMN migration across endothelium and colonic epithelial cells at a step subsequent to firm adhesion (*10*, *11*), suggesting that IAP functions in generation of an inflammatory response through effects not only on PMN activation, but also on the extravasation of PMNs.

We generated gene-targeted knockout mice deficient in IAP expression ($IAP^{-/-}$) (Fig. 1) to more clearly define the role of IAP in host defense against infection in vivo. To ensure that no functional fragments of IAP would be expressed, we targeted exon 2 (Fig. 1, A and B), the exon encoding both the predicted signal peptide cleavage site and the entire Ig domain, which is the target of all inhibitory monoclonal antibodies (mAbs) to IAP (*3*). Monoclonal antibodies recognizing the IAP Ig domain did not detect any IAP antigen on the surface of erythrocytes, bone marrow cells (Fig. 1C), or any other cells tested (*12*) from homozygote IAP-targeted mice. Likewise, no antigen was detectable in erythrocyte lysates of these mice with polyclonal antisera to IAP NH_2- or COOH-termini (Fig. 1D).

Despite the broad expression of IAP, IAP-deficient mice developed normally and were indistinguishable from their littermates by appearance, weight, fertility, and organ histology. No gross neurological abnormalities or excess morbidity or mortality were seen during 2 years of observation in a specific pathogen-free animal facility. Apart from a reduction in the $CD3^+$ fraction of peripheral lymphocytes, blood counts were normal (*13*, *14*). A gene dosage effect on IAP expression was observed, with protein on heterozygote cells reduced by ~40% compared with the wild type (Fig. 1). PMN surface expression of integrin chains β_2 (CD18), α_v (CD51), β_3 (CD61), and IgG Fc receptors (CD16 and CD32) on $IAP^{-/-}$ PMNs were identical to the heterozygote both before and after activation with phorbol 12-myristate 13-acetate (PMA) (*13*).

To assess the effect of IAP deficiency on host defense, we challenged mice with intraperitoneal injection of virulent *Escherichia coli* (O18:K1:H7) (*15*, *16*). The effect of IAP deficiency on survival in response to challenge with *E. coli* was marked. When challenged with 5×10^4 organisms intraperitoneally, all IAP-deficient mice died, whereas all their heterozygote littermates

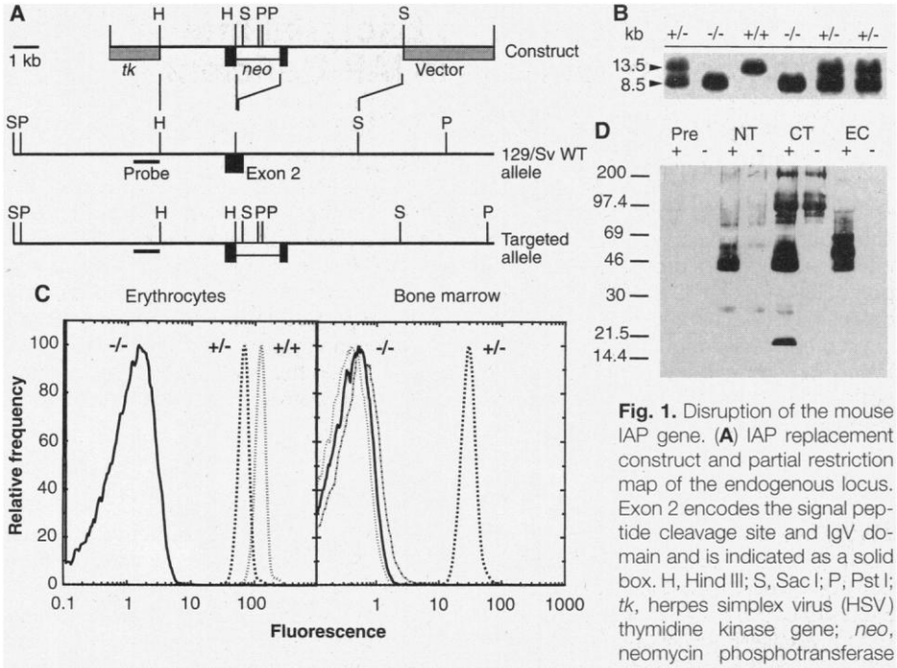

Fig. 1. Disruption of the mouse IAP gene. (**A**) IAP replacement construct and partial restriction map of the endogenous locus. Exon 2 encodes the signal peptide cleavage site and IgV domain and is indicated as a solid box. H, Hind III; S, Sac I; P, Pst I; *tk*, herpes simplex virus (HSV) thymidine kinase gene; *neo*, neomycin phosphotransferase gene; probe, IAP-specific probe used in screening (*22*); WT, wild type. (**B**) Southern (DNA) blot confirmation of the IAP mutation. The probe indicated in (A) was used to probe Sac I digests of tail DNA from mutant and nonmutant mice (genotype is indicated). This probe yields fragments of 8.5 and 13.5 kb, for the mutated and wild-type locus, respectively. (**C**) Flow cytometric assay of IAP surface expression on erythrocytes and bone marrow cells from $IAP^{-/-}$, $IAP^{+/-}$, and $IAP^{+/+}$ mice. Each curve represents results from one mouse. (Left) Erythrocytes from homozygote gene-targeted mice showed staining with anti-IAP (thick solid line) indistinguishable from that with negative control mAb (*24*). (Right) Bone marrow cells from $IAP^{-/-}$ mice (thick solid line) show staining with anti-IAP similar to $IAP^{-/-}$ or $IAP^{+/-}$ cells stained with negative control monoclonal antibody (thin solid line and thin dotted line, respectively). (**D**) Protein immunoblot of erythrocyte membrane lysates from wild-type (+) and homozygote gene-targeted mice (−) were probed with preimmune rabbit serum (Pre), polyclonal antiserum to the NH_2-terminus (NT), antiserum to the IAP-2 COOH-terminal cytoplasmic tail (CT), or mAb miap301 to the Ig domain of IAP (EC) (*25*). IAP migrates at ~46 kD (molecular sizes indicated to the left in kilodaltons). In addition, the CT-reactive antiserum detected a ~21-kD band in the wild-type lysate. This was probably a proteolytic fragment lacking the Ig domain and is not seen in the lysate of $IAP^{-/-}$ erythrocytes.

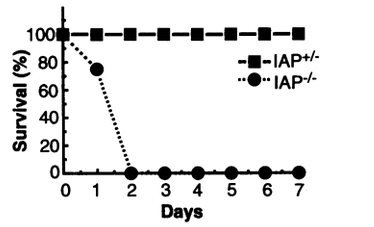

Fig. 2. Survival after intraperitoneal challenge with 5×10^4 *E. coli* in IAP-deficient ($IAP^{-/-}$) and heterozygote ($IAP^{+/-}$) 8-week-old female mice (*27*). Survival was assayed daily after challenge ($P = 0.008$, Fisher's exact test).

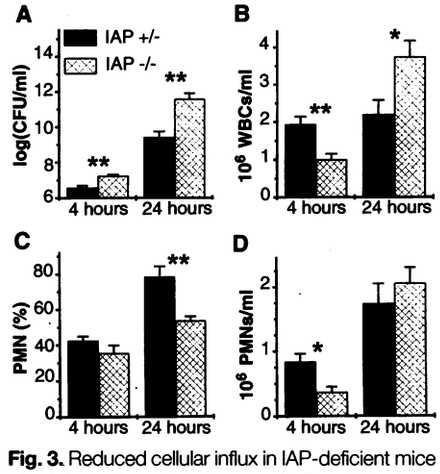

Fig. 3. Reduced cellular influx in IAP-deficient mice after intraperitoneal challenge with *E. coli*. Bacterial colony counts (**A**), total cell counts (**B**), and differential counts (**C**) were determined for peritoneal lavages of IAP-deficient mice and littermate heterozygote controls 4 and 24 hours after intraperitoneal challenge with *E. coli* (*28*). PMN counts (**D**) were calculated from cell count and differential count. Data are presented as mean ± SEM. Significance is shown as (**) for $P < 0.01$, and (*) for $P < 0.05$, as determined by the Wilcoxon-Mann-Whitney test. CFU, colony-forming units; WBC, white blood cells.

survived the infection (Fig. 2). This difference in survival was also evident when a 10-fold higher inoculum was used, although at this dose, some of the $IAP^{+/-}$ mice also died (*13*).

To determine how IAP deficiency impairs host defense, we examined the cellular infiltrate and bacterial colony counts 4 and 24 hours after *E. coli* challenge (Fig. 3). At 4 hours, the influx of both PMNs and other cells (mainly mononuclear leukocytes) was diminished in $IAP^{-/-}$ mice compared with $IAP^{+/-}$ littermates, demonstrating a defect in cell migration in the $IAP^{-/-}$ mice. At 24 hours the cellular infiltrate consisted almost exclusively of PMNs and macrophages. Although similar numbers of PMNs were recovered from both groups (Fig. 3D), lavages from $IAP^{-/-}$ mice contained significantly more macrophages (Fig. 3, B and C). Quantitation of bacterial colony-forming units revealed that a defect in the control of bacterial growth in IAP-deficient mice was already apparent 4 hours after challenge (Fig. 3A). At 24 hours, more than 100-fold more *E. coli* were recovered from the peritoneal cavities [and spleens (*13*)] of $IAP^{-/-}$ mice than from heterozygote controls, suggesting that the PMN defect resulted in a decreased ability to control infection (Fig. 3A). At this time, all $IAP^{-/-}$ mice showed more signs of severe infection than their littermates (hunched, ruffled fur, hypothermia, impaired ambulation, lethargy). Although the cellular infiltrate in the peritoneum of $IAP^{-/-}$ mice was not diminished at 24 hours, the interpretation of this result is complicated by the 100-fold higher bacterial burden in $IAP^{-/-}$ mice compared with control mice. Thus, PMN migration to an extravascular site of infection can occur in the absence of IAP, but migration is delayed and may never approach normal levels.

A large number of adhesion molecules have been identified that are involved in PMN migration from the blood stream into inflamed tissue. However, decreased PMN emigration is not always associated with a host defense defect as severe as IAP deficiency (*17*, *18*). For example, although there is a trend toward an increased incidence of bacteremia after intraperitoneal challenge with *Pseudomonas aeruginosa*, ICAM-1 deficiency had no effect on survival after challenge with either this pathogen or *E. coli* (*18*). This suggests that IAP deficiency may affect other aspects of PMN function. Monoclonal antibodies to IAP inhibit activation of PMNs by Arg-Gly-Asp–containing matrix proteins and their peptide analogs (*7*). Thus, we investigated the effect of IAP deficiency on PMN activation.

PMNs were purified from bone marrow of IAP-deficient mice and heterozygote or wild-type mice. Yields and cell morphology were similar. Control murine PMNs, like human PMNs, bound particles coated with the PMN β_3 ligand peptide KGAGDVA (*9*), up-regulated IgG Fc receptor–mediated phagocytosis in response to soluble peptide, and generated an oxidative burst in response to surface-bound peptide (Fig. 4) (*8*). In contrast, in IAP-deficient PMNs the β_3 integrin failed to bind ligand-coated beads efficiently (Fig. 4D), although expression of α_v and β_3 integrins was identical to expression in control mice (*13*). In the absence of IAP, PMNs did not respond to KGAGDVA for either oxidative burst (Fig. 4C) or Fc receptor–mediated phagocytosis (Fig. 4A), whereas in all cases the effector response of $IAP^{-/-}$ PMNs to control stimuli phorbol dibutyrate (PDBu) and formyl-Met-Leu-Phe (fMLP) was normal (Fig. 4A). This defect in activation could not be overcome by increasing the concentration of the activating peptide (Fig. 4B). High concentrations of KGAGDVA not only failed to activate but actually inhibited Fc receptor–mediated phagocytosis by $IAP^{-/-}$ PMNs (Fig. 4B).

The importance of β_2 integrins to PMN activation is well established (*19*). Expression of β_2 (*13*) and the binding of C3bi-opsonized particles by $IAP^{-/-}$ PMNs was normal (Fig. 4E). β_2-deficient PMNs fail to activate Fc receptor–mediated phagocytosis in response to PDBu and fMLP (*20*). The normal response of $IAP^{-/-}$ PMNs to these stimuli (Fig. 4A) shows that not only β_2 ligand binding but also β_2 signaling is intact in the absence of IAP. Thus, IAP deficiency specifically affects the β_3 integrin–generated activation signal, without direct consequences on either the effector functions themselves or on PMN activation through other pathways. This PMN phenotype is similar to anti-IAP–treated human PMNs (*7–9*).

In conclusion, IAP-deficient mice have a defect in host defense, probably secondary to both delayed PMN migration to the site of infection and to defective activation at that site. Because IAP both acts as a component of β_3 integrin signaling (*8*) and as a receptor for the ECM protein thrombospondin (*21*), IAP would be ideally suited to integrate signals from several matrix proteins to inform the PMNs that it is in tissue, rather than in the blood stream. Regulation of early, adhesive steps in the transendothelial migration process limits PMN extravasation to sites overlying inflammation. The role for IAP may be to regulate the final commitment to emigration from the vasculature and activation to full antibacterial activity. This suggests a more important

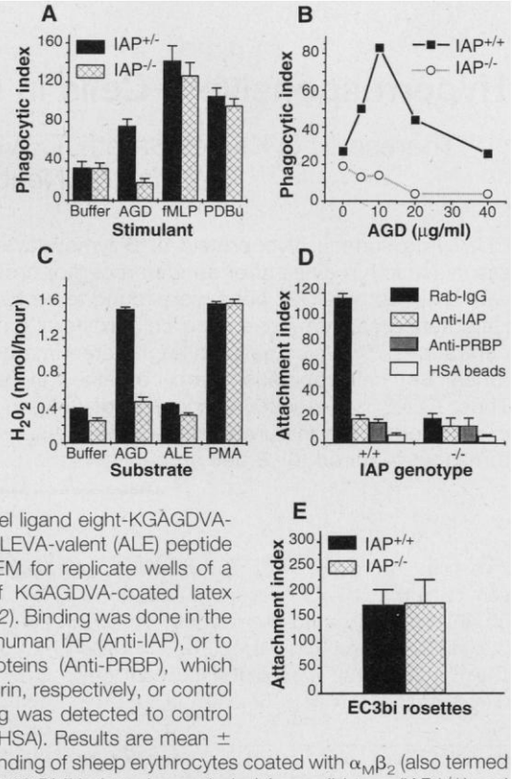

Fig. 4. In vitro phenotype of PMNs from IAP-deficient and heterozygote mice. (**A**) Phagocytosis of IgG-opsonized sheep red blood cells (*29*): baseline phagocytosis (buffer) or phagocytosis in response to various stimuli. Phagocytosis was stimulated with eight-KGAGDVA-valent peptide (AGD) (20 μg/ml) (*9*), PDBu (30 ng/ml), or 50 μM fMLP. Data are shown as mean ± SEM for five mice of each genotype. Results obtained with wild-type PMNs were very similar to those obtained with heterozygote cells in all assays. (**B**) Dose response of Fc receptor–mediated phagocytosis in response to stimulation with increasing concentrations of eight-KGAGDVA-valent peptide (*29*). IAP-deficient (open circles) and wild-type (filled squares) PMNs were compared. (**C**) Oxidative burst generated on a control surface in the absence (buffer) or presence of PMA (100 ng/ml) or on surfaces coated with the model ligand eight-KGAGDVA-valent (AGD) or with the inactive eight-KGALEVA-valent (ALE) peptide (L, Leu; E, Glu) (*31*). Data are mean ± SEM for replicate wells of a representative experiment. (**D**) Binding of KGAGDVA-coated latex beads (a PMN $\alpha_v\beta_3$ integrin model ligand) (*32*). Binding was done in the presence of polyclonal rabbit antiserum to human IAP (Anti-IAP), or to human placental Arg-Gly-Asp binding proteins (Anti-PRBP), which cross-react with murine IAP and PMN integrin, respectively, or control normal rabbit IgG (Rab-IgG) (*7*). No binding was detected to control beads coated with human serum albumin (HSA). Results are mean ± SEM for three mice of each genotype. (**E**) Binding of sheep erythrocytes coated with $\alpha_M\beta_2$ (also termed CD11b and CD18) ligand C3bi (EC3bi) per 100 PMNs (attachment index) from wild-type ($IAP^{+/+}$) and IAP-deficient ($IAP^{-/-}$) mice (*33*). Data are mean ± SEM for three mice per genotype.

role for PMN-ECM interactions in host defense against virulent organisms than was previously realized.

REFERENCES AND NOTES

1. J. D. Pollock *et al.*, *Nature Genet.* **9**, 202 (1995).
2. S. H. Jackson, J. I. Gallin, S. M. Holland, *J. Exp. Med.* **182**, 751 (1995).
3. F. P. Lindberg, H. D. Gresham, E. Schwarz, E. J. Brown, *J. Cell Biol.* **123**, 485 (1993).
4. F. P. Lindberg *et al.*, *J. Biol. Chem.* **269**, 1567 (1994).
5. E. J. Brown, L. Hooper, T. Ho, H. D. Gresham, *J. Cell Biol.* **111**, 2785 (1990).
6. M. I. Reinhold *et al.*, *J. Cell Sci.* **108**, 3419 (1995).
7. H. D. Gresham, J. L. Goodwin, P. M. Allen, D. C. Anderson, E. J. Brown, *J. Cell Biol.* **108**, 1935 (1989).
8. M.-J. Zhou and E. J. Brown, *J. Exp. Med.* **178**, 1165 (1993).
9. H. D. Gresham, S. P. Adams, E. J. Brown, *J. Biol. Chem.* **267**, 13895 (1992).
10. D. Cooper, F. P. Lindberg, J. R. Gamble, E. J. Brown, M. A. Vadas, *Proc. Natl. Acad. Sci. U.S.A.* **92**, 3978 (1995).
11. C. A. Parkos *et al.*, *J. Cell Biol.* **132**, 437 (1996).
12. Peripheral blood leukocytes, splenocytes, and fibroblasts (*13*).
13. F. P. Lindberg *et al.*, unpublished data.
14. A cohort of 9 to 21 mice of each IAP genotype was tested for peripheral blood/hemoglobin, platelet count, and white blood cell (WBC) count at 38 days of age, and for WBC count and PMN count at both 9 to 11 weeks and 1 year of age. Counts were not significantly different between the genotypes. The PMN counts at 9 to 11 weeks were 1.30 ± 0.25, 1.70 ± 0.23, and 1.62 ± 0.18 cells per nanoliter (mean ± SEM), for $IAP^{+/+}$, $IAP^{+/-}$, and $IAP^{-/-}$ mice, respectively.
15. A. S. Cross *et al.*, *J. Exp. Med.* **169**, 2021 (1989).
16. J. H. Lowrance, F. X. O'Sullivan, T. E. Caver, W. Waegell, H. D. Gresham, *ibid.* **180**, 1693 (1994).
17. T. N. Mayadas, R. C. Johnson, H. Rayburn, R. O. Hynes, D. D. Wagner, *Cell* **74**, 541 (1993); M. L. Arbones *et al.*, *Immunity* **1**, 247 (1994); J. E. Sligh Jr. *et al.*, *Proc. Natl. Acad. Sci. U.S.A.* **90**, 8529 (1993); D. C. Bullard *et al.*, *J. Clin. Invest.* **95**, 1782 (1995).
18. G. Sarman, S. B. Shappell, E. O. Mason Jr., C. W. Smith, S. L. Kaplan, *J. Infect. Dis.* **172**, 1001 (1995).
19. E. J. Brown and F. P. Lindberg, in *Blood Cell Biochemistry: Macrophages and Related Cells*, J. A. Horton, Ed. (Plenum, New York, 1993), vol. 5, pp. 279–306.
20. H. D. Gresham *et al.*, *J. Clin. Invest.* **88**, 588 (1991).
21. A. G. Gao, F. P. Lindberg, M. B. Finn, S. D. Blystone, W. A. Frazier, *J. Biol. Chem.* **271**, 21 (1996).
22. H. D. Gresham, C. J. Ray, F. X. O'Sullivan, *J. Immunol.* **146**, 3911 (1991).
23. J. A. Griffin and F. M. Griffin Jr., *J. Exp. Med.* **150**, 653 (1979).
24. A cDNA for mouse IAP (*3*) was used to screen a 129/Sv genomic library (Stratagene, LaJolla, CA). An overlapping set of genomic clones encoding the 5′-end of the cDNA up to the first two-thirds of the multiply membrane-spanning domain was assembled. An IAP replacement construct was generated by inserting the *neo*^{r} gene from pPol2neobpA (gift from P. Soriano) into exon 2, which encodes the signal peptide cleavage site and entire IAP IgV domain. This construct was electroporated into AB2.1 embryonic stem cells [P. Soriano, C. Montgomery, R. Geske, A. Bradley, *Cell* **64**, 693 (1991); M. R. Kuehn, A. Bradley, E. J. Robertson, M. J. Evans, *Nature* **326**, 295 (1987); A. P. McMahon and A. Bradley, *Cell* **62**, 1073 (1990)]. Digestion with Sac I and hybridization with the probe indicated was used to identify homologous recombinants. Multiple clones were isolated that correctly targeted the IAP gene, and injection of one of these resulted in germline transmission.
25. Mice were tail bled, and washed erythrocytes stained first with mAb miap301 to mouse IAP, then with fluorescein isothiocyanate–labeled secondary antibody and analyzed by flow cytometry. As a negative control, an isotype-matched mAb to keyhole limpet hemocyanine (KLH) was used. Single-cell suspensions of mouse bone marrow (from femurs and tibiae) were similarly analyzed, except that staining was done in the presence of excess human IgG (1 mg/ml) to block Fc receptor interactions.
26. Erythrocyte ghosts were prepared from 1 ml of mouse blood by lysis and washing in 5 mM tris-HCl (pH 8.0) and 1 mM phenylmethylsulphonyl fluoride. Equivalent amounts of protein were solubilized in nonreducing SDS sample buffer, electrophoresed on a 10% SDS-polyacrylamide gel, and reacted with a 1/500 dilution of polyclonal rabbit antibody to IAP cytoplasmic tail (*3*) or to the IAP NH_2-terminus [raised to KLH-conjugated pyro-QLLFSNVNSIEFTSC (single letter amino acid code: pyro-Q, pyro-Gln; L, Leu; F, Phe; S, Ser; N, Asn; V, Val; I, Ile; E, Glu; C, Cys)] followed by washing, incubation with peroxidase-labeled goat antibody to rabbit IgG, and detection by enhanced chemoluminescence (Amersham, Arlington Heights, IL).
27. *Escherichia coli* O18:K1:H7 (*12*) was passaged twice in C57BL/6J mice before use. IAP-deficient (n = 4) or littermate controls (+/−; control) (n = 5) from mice back-crossed five generations onto C57BL/6J were inoculated intraperitoneally with 5×10^4 bacteria in 100 μl of pyrogen-free saline and observed as described (*16*). Mice back-crossed for eight generations yielded similar results (*13*).
28. IAP-deficient mice (n = 7) back-crossed for eight generations onto C57BL/6J and heterozygote littermate controls (n = 5) were challenged with 3×10^4 *E. coli* O18:K1:H17 (see Fig. 2). After 4 hours, mice were anesthetized and killed, and 5-ml peritoneal lavages in sterile saline obtained as described (*16*). Similarly, IAP-deficient (n = 6) and control (n = 5) mice were challenged with 4.3×10^4, and after 24 hours total cell counts, differential counts, and colony-forming units of *E. coli* were assessed and PMN counts were calculated.
29. Sheep red blood cells (RBCs) opsonized with murine IgG2b antibody to sheep RBCs were prepared and incubated with murine bone marrow PMNs after a brief centrifugation as described (*22*). After lysis of extracellular targets, RBCs phagocytosed per 100 PMNs (phagocytic index) were determined (*22*).
30. Microtiter plates were coated with 50 μl of eight-KGAGDVA-valent peptide (150 μg/ml) and eight-KGALEVA-valent peptide (150 μg/ml) as described (*8*). Then 2×10^5 murine bone marrow PMNs were added per well and hydrogen peroxide production assayed after 60 min with a scopoletin-based fluorescence assay (*8*).
31. Fluorescent latex beads (1.3 μm) were coated with eight-KGAGDVA-valent peptide or HSA as described (*9*). Next 3×10^5 murine bone marrow PMNs were incubated 15 min at room temperature in 100 μl of Hanks' balanced salt solution with catalase, 0.1 mM fMLP, and either normal rabbit IgG (30 μg/ml), rabbit IgG to human IAP (30 μg/ml), or rabbit antiserum to human placental Arg-Gly-Asp binding integrins (*30*) at a dilution of 1:200. Then 45 μl of beads were added and the mixture incubated for 30 min at 37°C. Cells were washed twice, and PMN-bound fluorescent beads were counted under an ultraviolet microscope and expressed as beads bound per 100 cells (attachment index).
32. C3bi-coated sheep erythrocytes (EC3bi) were made by incubating 200 μl of sheep erythrocytes coated with rabbit IgM to sheep erythrocytes, 190 μl of veronal-buffered saline with dextrose, Ca^{2+} and Mg^{2+} (VBS), and 10 μl of C5-deficient mouse serum (absorbed with sheep erythrocytes) for 1 hour at 37°C followed by washing and resuspension in 400 μl of VBS (*23*). Then 200,000 PMNs in 50 μl of VBS, 50 μl of 100 μM fMLP in VBS, and 15 μl of EC3bi were pelleted briefly and resuspended, followed by incubation at 37°C for 30 min. The number of EC3bi rosetted per 100 PMNs was determined microscopically. No EC3bi are ingested under these conditions (*23*).

33. We thank M. Williams, I. Lorenzo, and L. A. Hurley for technical assistance and P. Soriano for reagents. Supported by NIH grants GM38330 (E.J.B.), AI32177 (A.L.B.), GM15483 (D.C.B.), the Howard Hughes Medical Institute (F.P.L. and A.L.B.), the American Arthritis Foundation (E.J.B. and F.P.L.), the Research Service of the Department of Veterans Affairs (H.D.G.), and the Monsanto–Washington University Agreement.

5 July 1996; accepted 22 August 1996

Hyperresponsive B Cells in CD22-Deficient Mice

Theresa L. O'Keefe, Gareth T. Williams, Sarah L. Davies, Michael S. Neuberger*

CD22 is a surface glycoprotein of B lymphocytes that is rapidly phosphorylated on cytoplasmic tyrosines after antigen receptor cross-linking. Splenic B cells from mice with a disrupted CD22 gene were found to be hyperresponsive to receptor signaling: Heightened calcium fluxes and cell proliferation were obtained at lower ligand concentrations. The mice gave an augmented immune response, had an expanded peritoneal B-1 cell population, and contained increased serum titers of autoantibody. Thus, CD22 is a negative regulator of antigen receptor signaling whose onset of expression at the mature B cell stage may serve to raise the antigen concentration threshold required for B cell triggering.

Antigen interaction with the B cell antigen receptor (BCR) triggers a cascade of protein tyrosine phosphorylation, which, depending on the maturational state of the B cell and on the nature of additional signals, leads to activation or death (*1*). CD22 is a B cell–restricted glycoprotein with an extracellular domain that binds glycoconjugates containing α 2,6-linked sialic acid (*2*). It associates with BCR and, after BCR cross-linking, becomes phosphorylated on cytoplasmic tyrosines, which leads to the recruitment of the haematopoietic phosphatase SHP-1 (*3*–*5*).

To study the role of CD22 in BCR-induced signaling, we generated mice with a

Medical Research Council Laboratory of Molecular Biology, Hills Road, Cambridge CB2 2QH, UK.

*To whom correspondence should be addressed.